

# Development and application of flexible substrate sensors in instantaneous heat flux measurement

XU Duo, GU JiaHua<sup>†</sup> & WU Song

Key Laboratory of High Temperature Gas Dynamics, Institute of Mechanics, Chinese Academy of Sciences, Beijing 100190, China

**A new type of sensor with the flexible substrate is introduced. It is applicable in measuring instantaneous heat flux on the model surface in a hypersonic shock tunnel. The working principle, structure and manufacture process of the sensor are presented. The substrate thickness and the dynamic response parameter of the sensor are calculated. Because this sensor was successfully used in measuring the instantaneous heat flux on the surface of a flat plate in a detonation-driven shock tunnel, it may be effective in measuring instantaneous heat flux on the model surface.**

heat flux, sensor, flexible substrate, hypersonic shock tunnel

The flow field around hypersonic aircraft flying in the aerosphere draws research interests in the field of aerodynamics, heat transfer and shock wave movement, etc.<sup>[1-5]</sup>. Meanwhile, the relevant discoveries are of fundamental importance in engineering applications, such as manned spacecraft, missile and rocket.

When a hypersonic aircraft flies in the aerosphere, a strong shock wave will be formed in front of its head. The air around the aircraft will be heated to several thousands of Kelvin, even ten thousands of Kelvin, under the effects of the shock wave. This is the reason why the Shenzhou spaceship looked like a fire ball during its reentry towards earth ground. Inside this flow field with high temperature, heat transfer and thermal radiation as well as other effects will increase the surface temperature of spacecraft to a significantly high temperature within very short time, which may result in fatal damage. Therefore, measuring heat flux across the model surface is important in ground simulation experiments on the hypersonic aircraft models.

At present, the thin film resistance-temperature sensor is popularly used measuring instantaneous heat flux. It is based on the linear relationship between resistance of the sensor and temperature, so the varieties of temperature can be measured through measuring the varieties of resistance. The thin film resistance temperature sensor is

made by depositing sub-micro Pt film, a temperature sensitive element, on the Pyrex or ceramic substrate using vacuum deposition technique. The sub-micro Pt film enables the sensor to have response time of microsecond, which makes it ideal for the hypersonic shock tunnel experiments whose valid experimental duration lasts about milliseconds. The sensor is installed at the targeted location on the model surface, and the active element of the sensor is part of the model surface. Thus the heat flux across the targeted area due to aero-heating can be measured by the sensor.

With the development of aeronautical technology, aircraft travels much faster, whose body shape and structure configuration become more complicated too. When measuring the heat flux on the complex surface area, limited by the size of the sensor, measurement points cannot be smaller. On the other hand, because the substrate of the thin film resistance temperature sensor is solid material, such as Pyrex and ceramics, the measurement surface of the sensor cannot be fully coincident with the model surface, which also brings adverse impact on the heat flux experimental results.

A sensor with the flexible substrate is able to solve

Received October 8, 2008; accepted December 10, 2008

doi: 10.1007/s11434-009-0182-7

<sup>†</sup>Corresponding author (email: [gu\\_jh@imech.ac.cn](mailto:gu_jh@imech.ac.cn))

the problem about measuring heat flux across a model surface with complex contour. This method not only makes the installation easier, but also makes the measurement face of the sensor fully attached to the model surface. Furthermore, it increases the number density of measuring points, which is helpful to obtaining the details of heat flux distribution in the crucial area of the model surface.

With the development of the micro-electro-mechanical-systems (MEMS) technology, some researchers, e.g. Lee et al.<sup>[6]</sup> and Mehregany et al.<sup>[7]</sup>, developed the shear force sensor and temperature sensor using flexible materials, but the temperature and speed of the flow field applicable to these sensors are low. Because Mach number, total pressure and total temperature of the flow field in a shock tunnel are high, there are rigid requirements on the scour resistance and stability of sensors. Thus, it is difficult to develop the flexible substrate sensor for the measurement of instantaneous heat flux in high total temperature, large heat flux and high enthalpy situation. No development reports and wind tunnel experimental results about this kind of sensor have been reported<sup>[8]</sup>.

## 1 Principle and manufacture process of the sensor

### 1.1 Measurement principle and theoretical model

The measurement principle of this kind of sensor depends on the linear relationship between resistance of metal and temperature  $\Delta R = \alpha_R \Delta T R$ , where  $\alpha_R$  is the resistance-temperature coefficient,  $R$  is the resistance of the sensor before the experiment,  $\Delta R$  is the varieties of the resistance of the sensor, and  $T$  is temperature<sup>[4,5]</sup>.

When the stationary current is applied on both sides of the sensor, there is a linear relationship between the resistance and voltage  $U = IR$ . The resistance of the sensor changes as the temperature changes, so the relevant change of voltage is  $\Delta U = U' - U = I \Delta R$ , where  $U$  is the voltage before temperature changes, and  $U'$  is the voltage after temperature changes. Thus the change of resistance can be measured by the change of voltage. The change of temperature on the model surface is  $\Delta T = \Delta U / I \alpha_R R = \Delta U / \alpha_R U$ .

The theoretical heat transfer model of the sensor can be simplified to one-dimensional semi-infinite medium

heat transfer model. This model is stable under the hypothesis: the metal film is thin enough that the thickness of the thin film and heat it absorbs could be ignored compared with the thickness of the substrate; the temperature of the thin film is the same as that of the sensor surface; within the experiment duration, the penetration depth of heat transfer into the substrate is so small that the substrate can be treated as a semi-infinite medium; the temperature gradient along the sensor surface is much smaller than that along the normal direction, so the heat transfer could be considered as one-dimensional.

Once the above hypothesis is satisfied, heat transfer across the sensor surface may be considered as one-dimensional semi-infinite medium heat transfer model. Heat flux can be calculated through the measured voltage by the following equation<sup>[8,9]</sup>:

$$q(t) = \frac{\sqrt{k\rho c}}{2\sqrt{\pi}\alpha_R E_0} \left[ \frac{2E(t)}{\sqrt{t}} + \int_0^t \frac{E(t) - E(\tau)}{(t - \tau)^{3/2}} d\tau \right], \quad (1)$$

where  $q(t)$  is heat flux,  $E_0$  is the original voltage between sides of the sensor,  $E(t)$  is the voltage at time  $t$ ,  $\alpha_R$  is the resistance-temperature coefficient of the sensor, and  $\sqrt{\rho ck}$  is the total heat identity parameter of the substrate material.

The sensor, like other sensors based on the resistance-temperature linear relationship, needs to be calibrated to obtain the resistance-temperature coefficient<sup>[10]</sup> before use.

### 1.2 Substrate material

The substrate material is the foundation of the flexible substrate heat flux sensor, which needs to have not only deforming capability and materials strength, but also excellent adiabatic performance.

Polyimide, due to its good performance and easy synthesis, has been applied widely in aeronautics, astronautics, microelectronic, nanotechnology, crystal, abrasion film and laser, etc. Polyimide has stable performance at  $-269 - 600^\circ\text{C}$ , including good adiabatic performance, whose heat transfer coefficient is  $2.87 \times 10^{-4}$  cal/(cm·s·°C). It also has good mechanical performance, with the tensile strength of the unfilled plastic >100 MPa. The tensile strength of the equal-benzene polyimide thin film is more than 170 MPa, and that of biphenyl polyimide reaches 400 MPa. Its elastic quantity is 3–4 GPa and that of fiber reaches 200 GPa. Certain

polyimide varieties do not dissolve in organic solvents, which prevent chemical etching.

### 1.3 Determining the thickness of the substrate material

As mentioned above, the theoretical model of this sensor is a one-dimensional semi-infinite heat transfer model. Under this hypothesis, the substrate needs to be semi-infinite along the heat transfer direction, but in reality, the substrate is not infinitely thick. In the experiment, if the thickness that heat transfer penetrates into the substrate material is small enough, the substrate thickness may be considered as semi-infinite. There are requirements on the thickness of the substrate of the sensor<sup>[9,11]</sup>.

In Figure 1, medium 1 is a metallic slab in thickness of  $\delta$ ; Medium 2 is the semi-infinite insulating substrate;  $\rho$ ,  $c$  and  $k$  are respectively the density, specific heat and coefficient of thermal conductivity of the material;  $\alpha$  is the thermal diffusivity related to  $\rho$ ,  $c$  and  $k$ , and defined as  $\alpha=k/\rho c$ ;  $x$  is the heat transfer depth of one-dimensional heat transfer. In Figure 1, subscript 1 refers to the parameters of metal material, and subscript 2 refers to the parameters of substrate material. According to the heat transfer model in Figure 1,

$$\frac{\partial^2 T_1}{\partial x^2} = \frac{1}{\alpha_1} \frac{\partial T_1}{\partial t}, \quad (2)$$

$$\frac{\partial^2 T_2}{\partial x^2} = \frac{1}{\alpha_2} \frac{\partial T_2}{\partial t}. \quad (3)$$

$$\text{At } x=0, \quad -k_1 \frac{\partial T_1}{\partial x} = q_s. \quad (4)$$

$$\text{At } x=\delta, \quad k_1 \frac{\partial T_1}{\partial x} = k_2 \frac{\partial T_2}{\partial x} \quad \text{and } T_1=T_2. \quad (5)$$

$$\text{At } x=\infty, \quad T_2=0. \quad (6)$$

From the above-mentioned hypothesis concerning the

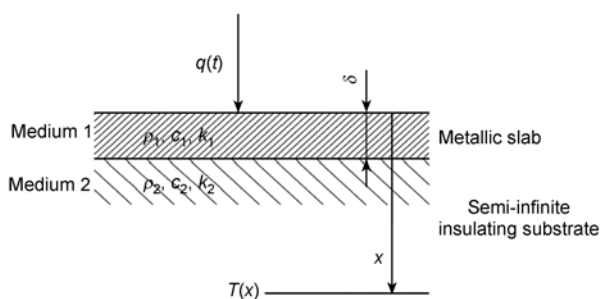


**Figure 1** One-dimensional semi-infinite heat transfer. heat transfer model and eqs. (2)–(6), the following

equations can be deduced:

$$T_x/T_s = e^{-\left(\frac{x}{\sqrt{4\alpha t}}\right)^2} - \sqrt{\pi} \frac{x}{\sqrt{4\alpha t}} \operatorname{erfc}\left(\frac{x}{\sqrt{4\alpha t}}\right), \quad (7)$$

$$q_x/q_s = \operatorname{erfc}\left(\frac{x}{\sqrt{4\alpha t}}\right). \quad (8)$$

When the temperature  $T_x$  and heat flux  $q_x$  at depth  $x$  reach 1% of the surface temperature  $T_s$  and surface heat flux  $q_s$ , as shown in Figure 2, from eqs. (7) and (8),

$$x_T = 3.16\sqrt{\alpha t}, \quad (9)$$

$$x_q = 3.74\sqrt{\alpha t}. \quad (10)$$

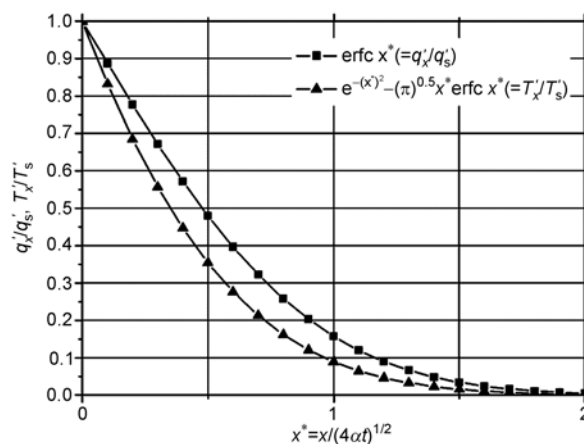


**Figure 2** Penetration of the thermal pulse into the substrate due to step function heat flux at the surface.

When the thickness of the substrate is bigger than  $x_T$  and  $x_q$ , the heat transfer model of the sensor satisfies the hypothesis on the one-dimensional semi-infinite heat transfer. The theoretical calculation results of several common materials that satisfy the hypothesis concerning the one-dimensional semi-infinite heat transfer are shown in Figure 3, and the heat transfer parameters are supposed to be constant in the calculation.

According to the analysis above, the penetration depth that meets the hypothesis for the one-dimensional semi-infinite heat transfer model can be calculated.

The relevant material parameters of polyimide are coefficient of heat conduction:  $k=2.87 \times 10^{-4}$  cal/(cm · s · °C),

density:  $\rho=1.42$  g/cm<sup>3</sup>,

specific heat:  $c=0.261$  cal/(g · °C),

coefficient of heat diffusivity:  $\alpha=k/\rho c=7.74378 \times 10^{-4}$  cm<sup>2</sup>/s.

From eqs. (9) and (10), under the condition of 20 ms

experimental duration, the thickness of the substrate material with the same assumption is calculated as follows:

$$x_T = 3.16\sqrt{\alpha t} = 3.16\sqrt{7.74378e-4 \text{ cm}^2/\text{s} \times 20\text{ms}} = 0.124 \text{ mm}, \quad (11)$$

$$x_q = 3.74\sqrt{\alpha t} = 3.74\sqrt{7.74378e-4 \text{ cm}^2/\text{s} \times 20\text{ms}} = 0.147 \text{ mm}. \quad (12)$$

These results show that the 0.18 mm thick polyimide film satisfies the relationships  $0.18 \text{ mm} > x_T$  and  $0.18 \text{ mm} > x_q$ . In other words, the heat transfer process occurring in the sensor satisfies the hypothesis during this 20 ms quasi-steady duration. In the calculation, the reference values of material properties are used, while the specification values from some manufacturers are better.

#### 1.4 Manufacture process of the sensor

The flexible substrate heat flux sensor was made by depositing a metal thin film on the flexible substrate as

sensitive element of the sensor. Due to the small size of the sensor and small thickness of the metal film, traditional depositing techniques could not meet the requirements, so it had to be made using the MEMS technique [12,13].

The dimension of the individual measurement point of the sensor is  $0.1 \text{ mm} \times 1 \text{ mm}$ , the space between adjacent points is  $0.5 \text{ mm}$ , and there are 10 points in an area of  $10.5 \text{ mm} \times 26 \text{ mm}$  (Figure 4). Except for the sensitive elements and pins of the sensor, the surface of other parts was deposited by polyimide using the photolithography technique in order to prevent the impact of heat transfer on the sensor and other parts.

#### 1.5 Calculation of dynamic response of the sensor

Since the shock tunnel experiment lasts few milliseconds, the sensor must have fast response time, which is very important to the flexible substrate heat flux sensor. The theoretical dynamic response time and rise time of the sensor are calculated as follows [14].

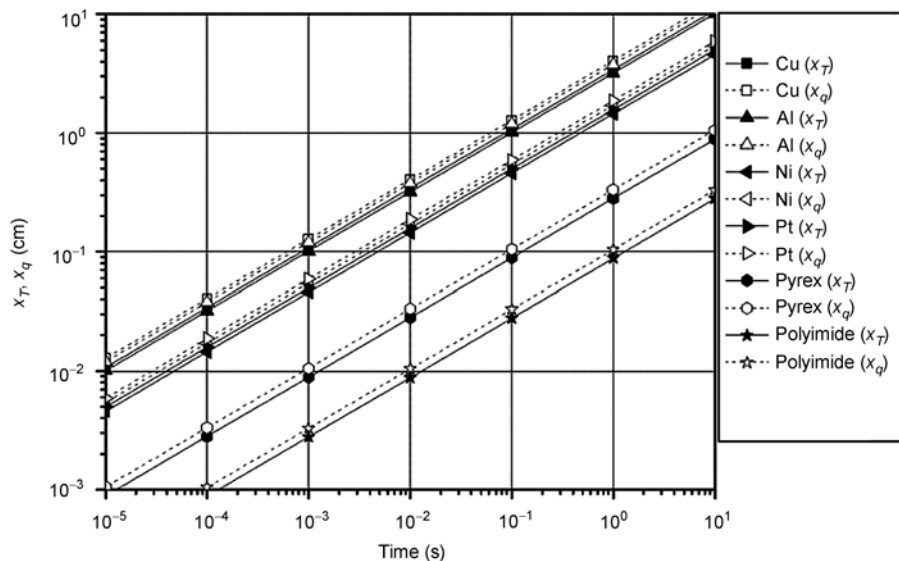


Figure 3 Temperature and heat flux at penetration depth  $x$  are 1% of those at the surface.

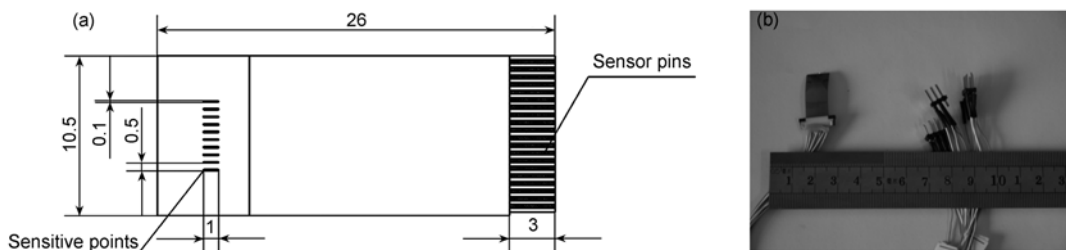


Figure 4 The size (a) and photo (b) of one piece of the sensor.

dynamic response time:

$$t_r = 0.5\delta^2/\alpha_1 = (0.5 \times 1 \mu\text{m}^2)/0.25 \text{ cm}^2\text{s}^{-1} = 0.01 \mu\text{s}, \quad (13)$$

dynamic rise time:

$$t_s = 3\tau = 3t_r/2.25 = 3 \times 0.01 \mu\text{s}/2.25 = 0.013 \mu\text{s}. \quad (14)$$

The calculation results show that the sensor has a fast response time at the sub-microsecond level, which makes it applicable to shock tunnel experiments. The experimental calibrations have not been finished. According to the empirical analysis, the experimental calibration results are usually one magnitude larger than the theoretical one.

## 2 Heat flux experiments on the flat plate surface

To verify the performance of the sensor, classical experiments in a shock tunnel were conducted, especially, to examine the dynamic response time and scour resistance. The flow field was generated through the two-direction detonation technique<sup>[15]</sup>, with Mach number 6.2, total pressure 20 bar and total temperature 3200 K. The experiment lasted 17 ms. The test model was a flat plate. The results were compared with the experimental results using the traditional thin film resistance-temperature sensor. Figure 5 shows the flat plate model and the sensor position pointed by a white arrowhead.

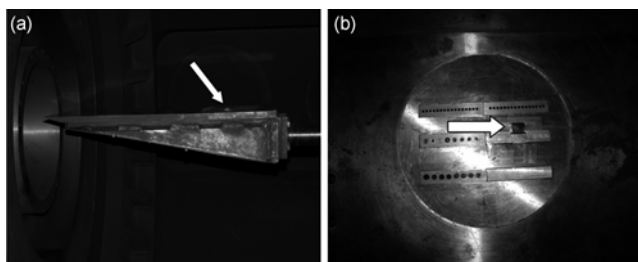


**Figure 5** The flat plate model and the sensor position. (a) Lateral view; (b) top view.

Figures 6 and 7 present the comparisons between the experimental curve of the flexible substrate heat flux sensor and that of the Pyrex substrate thin film resistance-temperature sensor in the flat plate heat flux experiments. The two curves agree very well. Correlation analysis further illustrates this point. Figure 8 shows the correlation curve between the experimental results of the flexible substrate heat flux sensor and that of the Pyrex substrate thin film resistance-temperature sensor. Tem-

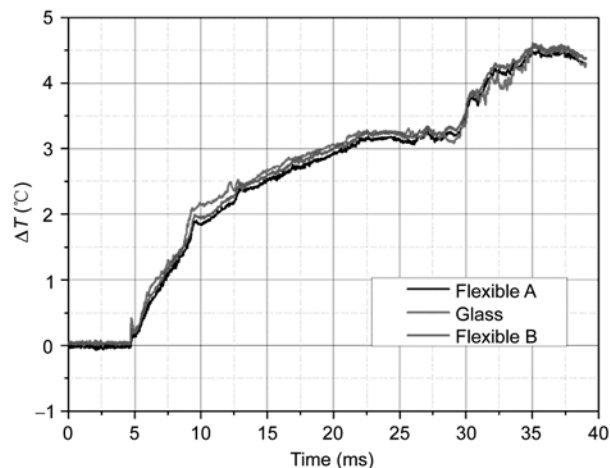


**Figure 6** The temperature curve of the flexible substrate heat flux sensor and that of the thin film resistance-temperature sensor.

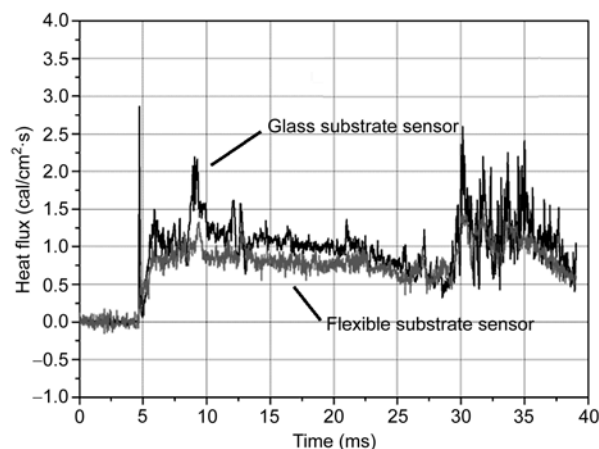


**Figure 7** The heat flux curve of the flexible substrate heat flux sensor and that of the thin film resistance-temperature sensor.

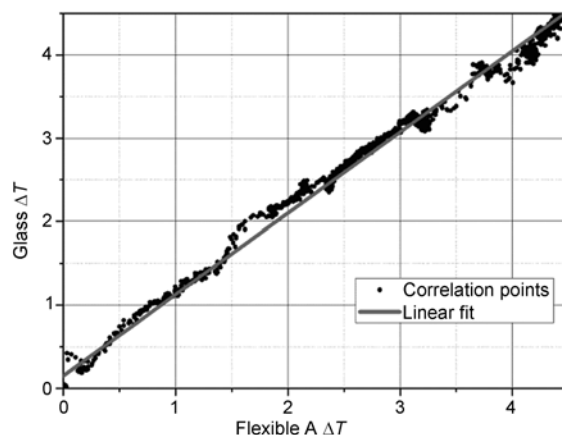


**Figure 8** Temperature correlation curves of the flexible substrate heat flux sensor and the Pyrex substrate thin film resistance-temperature sensor.

perature measured by two kinds of sensors rises with time, reflecting that the surface of the flat plate is being

heated in the flow field. If the responses of the two sensors are the same, there is a straight line crossing the origin point with a unity slope. In Figure 8, the calculated correlation coefficient is 0.997185, which justifies this linear relationship:

$$\gamma = \frac{\sum (x - \bar{x})(y - \bar{y})}{\sqrt{\sum (x - \bar{x})^2 \cdot \sum (y - \bar{y})^2}} = 0.997185. \quad (15)$$

Figure 9 shows the correlation curves of the experimental results from the two flexible substrate heat flux sensors. The correlation coefficient (such as eq. (16)) shows that the two flexible substrate heat flux sensors have nearly identical responses.

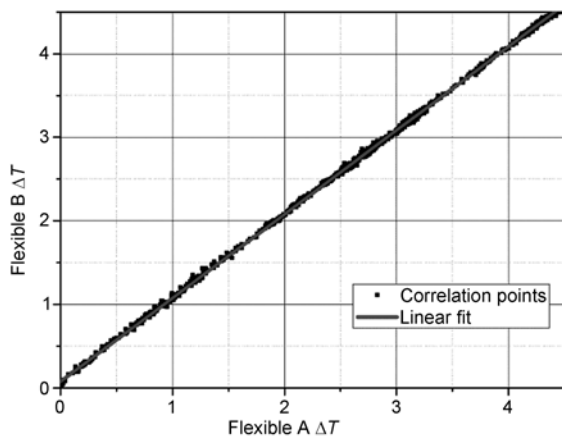


**Figure 9** Temperature correlation curves of the two flexible substrate heat flux sensors.

$$\gamma = \frac{\sum (x - \bar{x})(y - \bar{y})}{\sqrt{\sum (x - \bar{x})^2 \cdot \sum (y - \bar{y})^2}} = 0.999892. \quad (16)$$

### 3 Conclusions

A flexible substrate heat flux sensor was developed, and its good performance was validated in measuring the heat flux on a flat plate surface in the shock tunnel experiment. This sensor may be used in the instantaneous heat flux measurement in shock tunnel experiments. Because of the flexible substrate, the measurement surface of the sensor fits closely with the model surface, which enables it to be applied as a test model with complicated surface geometries. Also because of the small size of the sensor, being only 0.1 mm×1 mm, and the 0.5 mm space between measurement points, it may be used in multiple-point measurement in an area with a strong heat flux gradient, as well as in heat flux measurement in large areas. This sensor is still under an on-going development stage, and further investigation is necessary. For example, the manufacture process needs to be ameliorated and improved to meet the shock tunnel experimental requirements.

*The authors would like to acknowledge the help from the National Key Laboratory of Sensor Technology, Institute of Electronics, Chinese Academy of Sciences and Prof. Wang Shifen of Institute of Mechanics, Chinese Academy of Sciences.*

- 1 Zhao Y X, Yi S H, He L, et al. The experimental study of interaction between shock wave and turbulence. *Chin Sci Bull*, 2007, 52(10): 1297–1301 [\[DOI\]](#)
- 2 Teng H H, Jiang Z L. Gasdynamic characteristics of toroidal shock and detonation wave converging. *Sci China Ser G-Phys Mech Astron*, 2005, 48(6): 739–749 [\[DOI\]](#)
- 3 Cao W, Zhou H. Existence of shocklets in a two-dimensional supersonic mixing layer and its influence on the flow structure. *Sci China Ser A-Math*, 2001, 44(9): 1182–1188 [\[DOI\]](#)
- 4 Han Z Y, Wang Z Q, Yin X Z, et al. A new method of inclined interaction of a moving shock with head shock in double drive shock tube and shock wave tunnel. *Sci China Ser A-Math*, 1987, 30(1): 74–81
- 5 Han Z Y, Yin X Z. Two dimension shock wave dynamical equation set of moving flow. *Sci China Ser A-Math*, 1989, 32(4): 369–378
- 6 Lee G B, Huang F C, Lee C Y, et al. A new fabrication process for a flexible skin with temperature sensor array and its applications. *Acta Mech Sin*, 2004, 20(2): 140–145 [\[DOI\]](#)
- 7 Mehregany M, DeAnna G R, Reshotko E, et al. Microelectromechanical systems for aerodynamics applications. NASA Technical Report, ARL-TR-1113
- 8 Holden M S. A database of aerothermal measurements in hypersonic flow in building block experiments for CFD validation. 41st Aerospace Sciences Meeting and Exhibit, AIAA 2003-1137
- 9 Schultz D L, Jones T V. Heat-transfer measurements in short-duration hypersonic facilities. AGARD-AG-165
- 10 Xu D, Gu J H. Calibration system of thin film resistance thermometer used in hypersonic wind tunnel (in Chinese). National Symposium on Experiment Fluid Mechanics, 2007
- 11 Vidal R J. Model instrumentation techniques for heat transfer and force measurements in a hypersonic shock tunnel. Cornell Aeronautical Laboratory Report No. WADC T.N., 1956
- 12 Senturia D S. *Microsystem Design*. New York: Springer Publishing Corporation, 2001
- 13 Fraden J. *Handbook of Modern Sensors— Physics, Designs and Applications*. 3rd ed. New York: Springer Publishing Corporation, 2004
- 14 Fan S C. *Sensor Technology and Its Applications* (in Chinese). Beijing: Beijing University of Aeronautics and Astronautics Press, 2004
- 15 Chen H, Feng H, Yu H R. Double detonation drivers for a shock tube/tunnel. *Sci China Ser G-Phys Mech Astron*, 2004, 47(4): 502–512 [\[DOI\]](#)